



# Synthesis of carbon nanorods by reduction of carbon bisulfide

Zhengsong Lou\*, Minglong He, Dejian Zhao, Zhongchun Li, Tongming Shang

Laboratory of Precious Metal Processing Technology and Application, School of Applied Chemistry, Jiangsu Teachers University of Technology, Yu Ying Road 2, Changzhou 213001, PR China

## ARTICLE INFO

Article history:  
Available online 17 July 2010

Keywords:  
Nanostructure  
Chemical synthesis  
N<sub>2</sub> physisorption  
Carbon nanorods  
Scanning electron microscopy  
X-ray diffraction

## ABSTRACT

Carbon nanorods are synthesized at large scale by the reduction of carbon bisulfide at 600 °C. Moreover, novel Y-junction carbon nanorods are detected in the samples. The X-ray power diffraction pattern indicates that the products are hexagonal graphite. Scanning electron microscopy, transmission electron microscopy, high-resolution transmission electron microscopy and N<sub>2</sub> physisorption studies show that carbon nanorods predominate in the product. Based on the supercritical carbon bisulfide system, the possible growth mechanism of the carbon nanorods was discussed. This method provides a simple and cheap route to large-scale synthesis of carbon nanorods.

© 2010 Elsevier B.V. All rights reserved.

## 1. Introduction

Carbon nanomaterials have attracted great interests in the past decades, especially after the detection of fullerenes [1]. The structures, texture and diversity of various carbon nanomaterials such as carbon nanoparticles [2], nanotubes [3], carbon nanorods [4], onions [5], nanowires [6] and nanofibers [7] were observed thereafter [1]. Understanding their properties and exploring their promising application have led to a great increase of research worldwide. The nano-meter carbon material is expected to behave like semiconductor with relatively large band gap. For example, carbon nanoparticles are of interests not only for fundamental studies of mechanical and electric properties, but also for various potential applications such as fillers [8], high-performance electrode materials in batteries [9]. Carbon nanorods have largely been applied in anodic materials of batteries because of their performance [10]. Up to now, various methods have been demonstrated for the synthesis of carbon nanorods, which include the arc discharge method [11], the chemical vapor deposition [12], the template methods [13], the electron beam-induced route [14] and the catalytic copyrolysis method [15].

Recently, we have been focusing on the synthesis of diamond and carbon-based materials by the reduction of carbon dioxide and carbonate with alkali metals [16–19]. Because of similar chemical and physical properties (polarity, supercritical phase, etc.) of carbon bisulfide and carbon dioxide, we tentatively try to synthesize carbon materials by the reduction of carbon bisulfide. In this study,

we report a method for synthesizing carbon nanorods on a large scale using the reaction of carbon bisulfide with metallic lithium in a stainless autoclave at 600 °C. The reaction can be formulated as follows:



We call this route the carbon bisulfide thermal reduction process, in which carbon bisulfide is used as the carbon source and Li is used as the reductant. Based on the field emission scanning electron microscope and transmission electron microscope analysis, the carbon nanorods account for about 80% of the carbon product, and the rest are graphite and amorphous carbon. In addition, various shaped Y-junction carbon nanorods are also found in the product.

## 2. Experimental

In this method, the reaction was carried out in a stainless steel autoclave (16 mL). If it is not specifically mentioned, most of the reactions were conducted at 600 °C. In a typical preparation, 12.0 mL CS<sub>2</sub> and 1.2 g of metallic Li were used, and they were placed in a stainless autoclave at room temperature. The vessel was then immediately closed tightly and heated up to 600 °C, and maintained at this temperature for 10 h. The reaction took place at an autogenic pressure depending on the reactant amount added. After cooling down to room temperature, the solid product was collected and treated in 6.0 mol/L HCl aqueous solution at 80 °C for 6 h to remove Li<sub>2</sub>S and iron based materials from the autoclave. A microfilter was used to collect the precipitate that was then washed with ethanol and dried in air, yielding about 0.49 g of product.

The X-ray diffraction (XRD) analysis was performed using a Rigaku (Japan) D/max-γA X-ray diffractometer equipped with graphite monochromatized Cu Kα radiation (λ = 1.54178 Å). The morphology of the samples was observed on a field emission scanning electron microscope (FESEM) (JEOL-6300F, 15 kV). Transmission electron microscopic (TEM) images and electron diffraction (ED) patterns were taken on a Hitachi H-800 transmission electron microscope. The microstructure of carbon nanorods was analyzed by high-resolution transmission electron microscopy (HRTEM), which was performed on a JEOL-2010 transmission electron microscope

\* Corresponding author. Tel.: +86 519 6999842; fax: +86 519 6999516.  
E-mail address: [lzs@jstu.edu.cn](mailto:lzs@jstu.edu.cn) (Z. Lou).

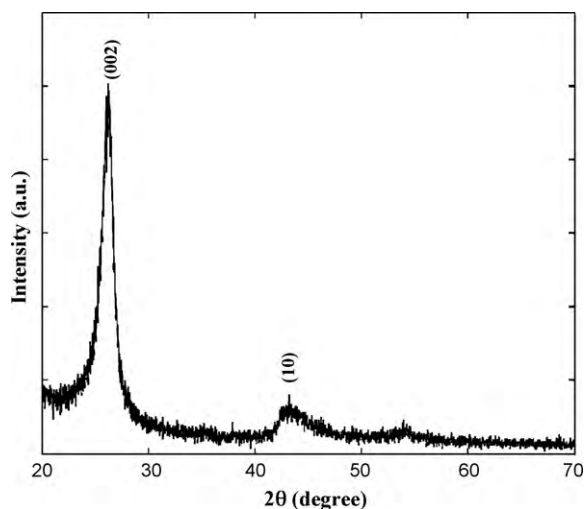


Fig. 1. XRD pattern of the products after treatment by HCl aqueous solutions.

using an accelerating voltage of 200 kV.  $N_2$  adsorption–desorption studies were carried out at 77 K with a static volumetric instrument Autosorb-1 (Quantachrome) to examine the porous properties of the sample. Samples were pretreated by out-gassing in vacuum at 200 °C for at least 5 h, and the pore size distribution (PSD) was evaluated from the desorption isotherms using the BJH method [20].

### 3. Results and discussion

Fig. 1 shows the XRD pattern of the sample after treated with 6.0 mol/L HCl aqueous solution. It contains characteristic diffraction peaks, indexed with 002 and 10, respectively, which corresponds to the hexagonal graphite phase (PDF cards, JCPDS 41-1487). Moreover, the broad (10) diffraction originates from a two-dimensional lattice. It can also be conformed by the HRTEM image of the sample.

Figs. 2 and 3 are FESEM and TEM images of carbon nanorods, respectively. The FESEM images show that there are large numbers of carbon nanorods in the sample, and the diameter of carbon nanorods ranges from 40 nm to 140 nm. Fig. 2b is the enlarged image of the rectangle area shown in Fig. 2a. Carbon nanorods can be clearly seen, indicating the large quantity of carbon nanorods obtained via this approach. The TEM images of the product reveal that the diameter of carbon nanorods is about 40–150 nm, and the lengths of carbon nanorods are in the range from hundreds of nanometers to several micrometers, which are in agreement with the result of FESEM observations. Fig. 3a is a typical TEM image of the carbon nanorods, and the selected area electron diffraction (SAED) pattern of the nanorods shows a pair of small but strong arcs corresponding to (002) (in Fig. 3d). The broadening of the diffraction ring is observed due to the rolling of graphitic layers. It should be noted that appreciable amount of various shaped Y-junction carbon nanorods (~10% based on TEM images) are observed in the products, which are shown in Fig. 3b and c. The SAED pattern (in Fig. 3e) of a junction of Y-like carbon nanorods exhibits four small but strong arcs for 002, which imply the orientation of the 002 planes in the junction of carbon nanorods. The results suggest that the junction is formed by the curvature caused by different carbon rings. These observations are consistent with previous report [21].

A more detailed investigation of as-prepared products was carried out by HRTEM. The HRTEM images show the irregular graphite layers are almost perpendicular to electron beam and their inter-layer spacing is about 0.34 nm, which is typical for the (002) lattice distance in hexagonal carbon. These graphite layers typically form multiwall structures and create complex morphologies, consisting of the combination of straight domains, bent walls, and multiwall circular shape (Fig. 4a and b).

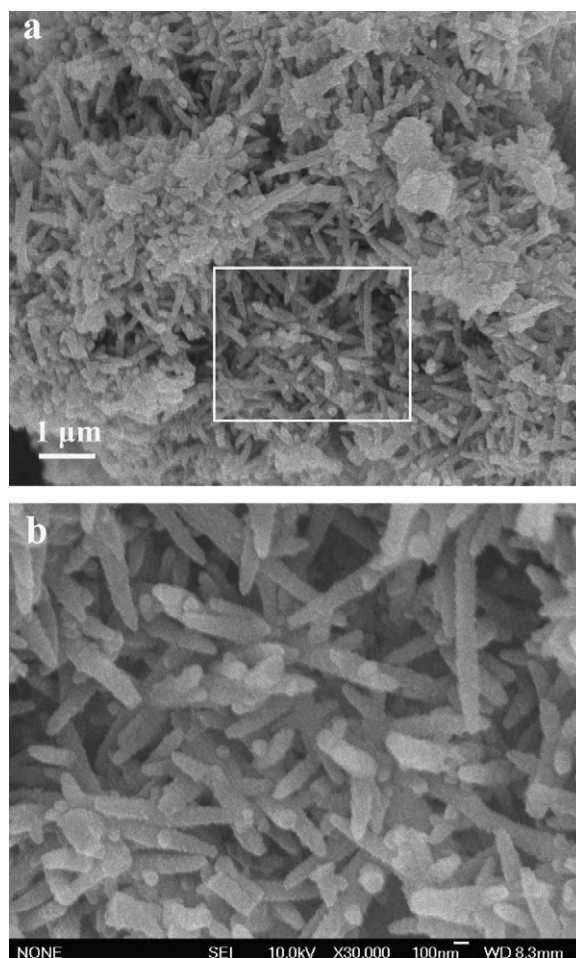
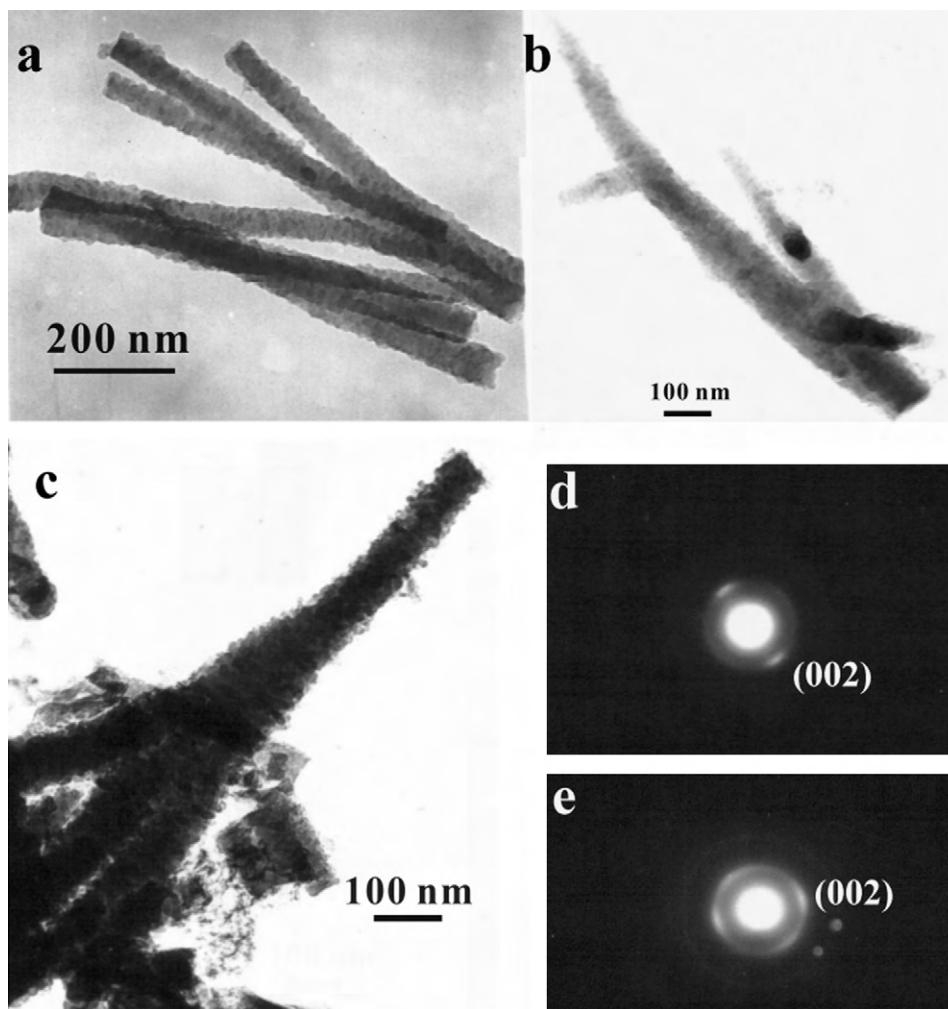


Fig. 2. FESEM image of the as-prepared product: (a) FESEM image of carbon nanorods and (b) the enlarged image of the rectangle area shown in (a).

The results of FESEM, TEM and  $N_2$  physisorption are complementary with respect to probing the structural integrity of the product. The images of FESEM and TEM can be used to observe the subtle portion of the material while  $N_2$  physisorption gives a picture of the overall porosity of the material. The  $N_2$  adsorption–desorption isotherm and PSD of the product are presented in Fig. 5a and b. The isotherms of the sample appears typically in Type IV characteristic, according to the IUPAC classification, with hysteresis loops initiating from the medium relative pressures ( $P/P_0 \sim 0.40$ ), and closing near  $P/P_0 \sim 1$ . BJH cumulative desorption surface area is  $74.42 \text{ m}^2 \text{ g}^{-1}$  and BJH cumulative desorption pore volume is  $14.26 \text{ cm}^3 \text{ g}^{-1}$ .

Pore size distributions of the carbon nanorods can be seen intuitively in Fig. 5b. The primary mesopores are found of a size of around 3.9 nm, accompanied with pore size of 1.7 nm, 2.2 nm, 2.6 nm, 3.0 nm and 6.2 nm by desorption BJH method. In the light of Cheng and coworkers research [22], there are more mesopores corresponding to the size of 3–4 nm, which demonstrates the products might contain MWNT, but samples exhibit relatively low pore volumes, these prove that the quantity of MWNT is small and main products are carbon nanorods, it has been further confirmed by FESEM and TEM results. There are no aggregated pores, which demonstrate carbon nanorods conglomerate compactness as indicated by FESEM image in Fig. 2.

The carbon nanorods with relatively high surface areas are expected to have similar chemical properties of carbon nanotubes, which might find potential applications such as catalyst carriers, lubricants and hydrogen storage materials [23]. In addition, the car-



**Fig. 3.** TEM micrographs of carbon nanorods: (a) TEM image of the typical carbon nanorods; (b and c) carbon nanorods with multiple Y-junctions; (d) selected area electron diffraction pattern of the carbon nanorods; (e) selected area electron diffraction pattern of the junction of Y-junction carbon nanorods.

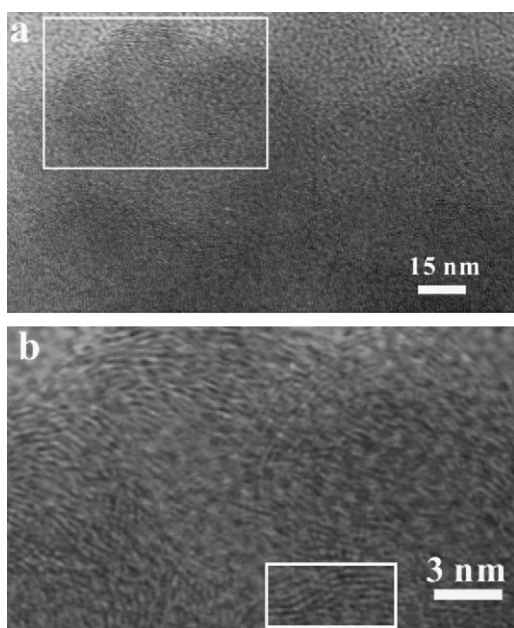


**Fig. 4.** HRTEM pictures of the product: (a) HRTEM micrograph of a typical carbon nanorod and (b) the magnified high-resolution image of the boxed regions in (a).

bon nanorods with various shaped Y-junctions can be used to study the intrinsic electron transport properties of carbon nanomaterials and build blocks of nanoelectronics [24].

It is not clear whether this reaction is catalyzed by any of the constituents of the stainless steel cell. To further examine the catalytic role of the stainless steel wall, a reaction was carried out in a copper cell under the same experimental conditions. The same products were obtained. Independent of nanorods formation on the wall

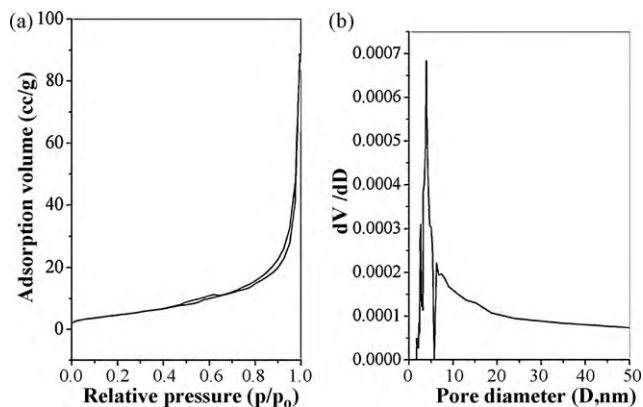


**Fig. 5.** Nitrogen physisorption results of the carbon nanorods: (a) adsorption/desorption isotherms and (b) pore size distributions.

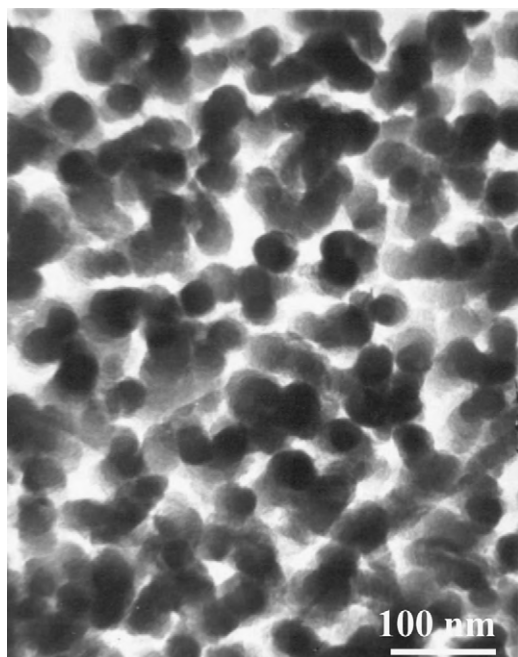


Fig. 6. TEM micrograph of the sample produced by the reaction at 600 °C for 5 h.

materials of the reaction cell makes us rule out the possibility that metal atoms of the wall catalyzed the formation of nanorods. When the reaction was conducted at 600 °C for 2 h, the main products are graphite and amorphous carbon. When the reaction is carried out at 600 °C for 5 h, The TEM image (Fig. 6) indicates that a large amount of the carbon nanoparticles with diameter of 30–40 nm formed in the as-synthesized sample and carbon nanorods are made up of small carbon nanoparticles and the length of carbon nanorods is about 60–150 nm. Also in a reaction at 600 °C for 10 h without the addition of lithium, it was found that only amorphous carbon was formed; suggesting nanorods formation is related to the reduction of CS<sub>2</sub> by metallic Li.

The metallic lithium melts at 180.5 °C and its boiling temperature is 1342 °C. The density of metallic lithium is 0.534 g/cm<sup>3</sup>, but the density of carbon bisulfide is 1.263 g/cm<sup>3</sup>, so the molten metallic lithium floats on the surface of carbon bisulfide. The critical point of carbon bisulfide is characterized by the pressure and temperature  $P_c = 75$  atm and  $T_c = 546$  K, respectively. The pressure of reaction system at 600 °C is about 820 atm, which indicates CS<sub>2</sub> being in supercritical state, so the gas and liquid phases merge into a single supercritical phase, which serves as a novel media for chemical reactions. Based on our experimental conditions and results, we describe a possible growth mechanism of the carbon nanorods. In the supercritical CS<sub>2</sub> system, liquid Li might form a nanoscale rough surface with nanoprotusions (we call nanoprotusions nanodroplets) at the growth temperature. The nanodroplets take the roles both as reductant for CS<sub>2</sub> reduction to carbon and as templates for the growth of carbon nanorods. It is suggested that molten lithium floating on the surface of carbon bisulfide, form many Li nanodroplets, and CS<sub>2</sub> molecules are reduced on Li droplets, resulting in the formation of first carbon nanoparticle. After the depletion of first droplet, under which a new Li droplet will be produced, second carbon nanoparticle will form by the reduction of CS<sub>2</sub> molecules on it. This process is going on one by one, a lot of carbon nanoparticles fitted together form carbon nanorod. Because the nanodroplets have a continued liquid lithium background, carbon nanorods interlinked by carbon nanoparticles as long as several

micrometers are produced. As the reaction proceeds, the amount of carbon bisulfide decreases, and molten metallic lithium falls. Due to the low mass metal with relatively weak metallic bonds and under the influence of gravitation of lithium and supercritical CS<sub>2</sub>, Li nanodroplet could form forfication on which a Y-junction carbon nanorod might grow. Because the number of forfication, the situation of forfication and the size of a new Li droplet are different, they would form various shaped Y-junction carbon nanorods. These are consistent with our experimental results, of course, due to the complexity of the experimental process, the exact formation mechanism of carbon nanorods still needs further research.

#### 4. Conclusions

In summary, carbon nanorods have been successfully synthesized at high yield by reduction of carbon bisulfide with metallic lithium at 600 °C. FESEM, TEM, HRTEM, and N<sub>2</sub> isotherm experiments reveal the morphology, size and fine structure of the product. Many various shaped Y-junction carbon nanorods were also found to present in the product. It is expected further work could lead to large-scale preparation of Y-junction carbon nanorods, which might be significant to the basic building units for nanoelectronic devices. Because of its simplicity and high yield, this process could be scaled up for industrial production of carbon nanorods with novel structure.

#### Acknowledgement

The authors gratefully acknowledge informative discussions with Professor Qianwang Chen.

#### References

- [1] H.W. Kroto, J.R. Heath, S.C. O'Brien, R.F. Curl, R.E. Smalley, *Nature* 318 (1985) 162–163.
- [2] J. Yu, J. Ahn, Q. Zhang, S.F. Yoon, Rusli, Y.J. Li, B. Gan, K. Chew, K.H. Tan, *J. Appl. Phys.* 91 (2002) 433–436.
- [3] S. Iijima, *Nature* 354 (1991) 56–58.
- [4] X.J. Wang, J. Lu, Y. Xie, G.A. Du, Q.X. Guo, S.Y. Zhang, *J. Phys. Chem. B* 106 (2002) 933–937.
- [5] W. Kratschmer, L.D. Lamb, K. Fostiropoulos, D.R. Huffman, *Nature* 347 (1990) 354–358.
- [6] Y.H. Tang, N. Wang, Y.F. Zhang, C.S. Lee, I. Bello, S.T. Lee, *Appl. Phys. Lett.* 75 (1999) 2921–2923.
- [7] Y. Chen, S. Patel, Y.G. Ye, S.T. Shaw, L.P. Luo, *Appl. Phys. Lett.* 73 (1998) 2119–2121.
- [8] A. Laforge, P. Simon, J.F. Fauvarque, M. Mastragostino, F. Soavi, J.F. Sarrau, P. Lailier, M. Conte, E. Rossi, S. Saguatti, *J. Electrochem. Soc.* 150 (2003) A645–A651.
- [9] R. Dominko, M. Gaberscek, J. Drogenik, M. Bele, J. Jamnik, *Electrochim. Acta* 48 (2003) 3709–3716.
- [10] S.H. Yoon, C.W. Park, H.J. Yang, Y. Korai, I. Mochida, R.T.K. Baker, N.M. Rodriguez, *Carbon* 42 (2004) 21–32.
- [11] Y.Q. Liu, W.P. Hu, X.B. Wang, C.F. Long, J.B. Zhang, D.B. Zhu, D.S. Tang, S.S. Xie, *Chem. Phys. Lett.* 331 (2000) 31–34.
- [12] L. Thien-Nga, K. Hernadi, L. Forro, *Adv. Mater.* 13 (2001) 148–150.
- [13] F. Kleitz, S.H. Choi, R. Ryoo, *Chem. Commun.* 17 (2003) 2136–2137.
- [14] K.H. Chen, C.T. Wu, J.S. Hwang, C.Y. Wen, L.C. Chen, C.T. Wang, K.J. Ma, *J. Phys. Chem. Solids* 62 (2001) 1561–1565.
- [15] G.F. Zou, J. Lu, D.B. Wang, L.Q. Xu, Y.T. Qian, *Inorg. Chem.* 43 (2004) 5432–5435.
- [16] Z.S. Lou, Q.W. Chen, Y.F. Zhang, W. Wang, Y.T. Qian, *J. Am. Chem. Soc.* 125 (2003) 9302–9303.
- [17] Z.S. Lou, Q.W. Chen, Y.F. Zhang, Y.T. Qian, W. Wang, *J. Phys. Chem. B* 108 (2004) 4239–4241.
- [18] Z.S. Lou, Q.W. Chen, W. Wang, Y.F. Zhang, *Carbon* 41 (2003) 3063–3067.
- [19] Z.S. Lou, Q.W. Chen, J. Gao, Y.F. Zhang, *Carbon* 42 (2004) 229–232.
- [20] E.P. Barrett, L.G. Joyner, P.P. Halenda, *J. Am. Chem. Soc.* 73 (1951) 373–380.
- [21] C.N.R. Rao, A. Govindaraj, *Acc. Chem. Res.* 35 (2002) 998–1007.
- [22] Q.H. Yang, P.X. Hou, S. Bai, M.Z. Wang, H.M. Cheng, *Chem. Phys. Lett.* 345 (2001) 18–24.
- [23] M. Rzepka, P. Lamp, M.A. Casa-Lillo, *J. Phys. Chem. B* 102 (1998) 10894–10898.
- [24] J. Li, C. Papadopoulos, J. Xu, *Nature* 402 (1999) 253–254.